Iran J Sci Technol Trans Sci (2017) 41:1109–1121
https://doi.org/10.1007/s40995-017-0238-5

RESEARCH PAPER

A New Approach for Numerical Solution of Modified Korteweg-de Vries Equation

Turgut Ak[1] · S. Battal Gazi Karakoc[2] · Anjan Biswas[3,4]

Received: 3 February 2016 / Accepted: 2 March 2017 / Published online: 4 April 2017

Abstract In this paper, a lumped Galerkin method is applied with cubic B-spline interpolation functions to find the numerical solution of the modified Korteweg-de Vries (mKdV) equation. Test problems including motion of single solitary wave, interaction of two solitons, interaction of three solitons, and evolution of solitons are solved to verify the proposed method by calculating the error norms L_2 and L_∞ and the conserved quantities mass, momentum and energy. Applying the von-Neumann stability analysis, the proposed method is shown to be unconditionally stable. Consequently, the obtained results are found to be harmony with the some recent results.

Keywords Modified KdV equation · Galerkin method · Solitary waves · Soliton · B-spline

Mathematics Subject Classification 41A15 · 65L60 · 76B15 · 76B25 · 35C08

✉ Turgut Ak
akturgut@yahoo.com

1 Department of Transportation Engineering, Faculty of Engineering, Yalova University, 77100 Yalova, Turkey

2 Department of Mathematics, Faculty of Science and Art, Nevsehir Haci Bektas Veli University, 50300 Nevsehir, Turkey

3 Department of Mathematical Sciences, Delaware State University, Dover, DE 19901-2277, USA

4 Department of Mathematics, Faculty of Science, King Abdulaziz University, Jeddah 21589, Saudi Arabia

1 Introduction

The dynamics of shallow water waves is one of the most popular areas of research in the fields of fluid mechanics and nonlinear evolution equations. There are several equations that govern this dynamics. These are Korteweg-de Vries (KdV) equation (Korteweg and de Vries 1895; Triki et al. 2016; Wazwaz 2016; Dyachenko et al. 2016), Boussinesq equation (Wazwaz 2008; Siddigi and Arshed 2014; Greenwood et al. 2016; Ueckermann and Lermusiaux 2016), Kawahara equation (Haq et al. 2010; Karakoc et al. 2014a), Peregrine equation (Girgis et al. 2010), Benjamin–Bona–Mahony equation (Biswas 2010; Wazwaz and Triki 2011; Vaneeva et al. 2015; Gheorghiu 2016) and several many others (Karakoc et al. 2014a, b; Rashidi et al. 2009a, b; Shukla et al. 2014). All of these equations stem from Euler's equation or rather Navier–Stokes equation in fluid dynamics. However, two-layered flow along lake shores and beaches are also modeled by Gear–Grimshaw model (Biswas and Ismail 2010; Triki et al. 2014), Zhareamogoddam model, Bona–Chen model (Biswas et al. 2013) and the other models.

With all of these varieties of models, there are several papers that reported analytical results. These covered soliton solutions, shock wave solutions, rogue wave solutions, soliton perturbation theory, stability analysis, quasi-stationary solutions, and several other aspects. What is visibly missing from this plethora of papers is a deep-down numerical analysis of these model equations that provide visual effects and thus appealing to the eye rather than applied analysis. However, there are a limited number of numerical studies in the literature about the mKdV equation. The explicit solutions to the higher order modified Kortewegde Vries equation with initial condition are calculated using the Adomian decomposition method (Kaya

2005). The equation is numerically solved using a new algorithm based on the finite element approach applying Galerkin's method with quadratic spline interpolation functions by Biswas and Raslan (2011). The equation is numerically solved using the finite-difference method. An energy conservative finite-difference scheme was proposed. Accuracy and stability of the difference solution were proved by Raslan and Baghdady (2015). This paper, therefore, carries out a detailed numerical study of the modified KdV equation that is another version of KdV equation (Triki and Wazwaz 2009; Wazwaz 2012; Wazwaz and Xu 2015; Dutykh and Tobisch 2015; He and Meng 2016). Moreover, better numerical results from earlier results in the literature are obtained.

This paper employs a lumped Galerkin method based on cubic B-spline interpolation functions to solve the mKdV equation. The proposed method is shown to represent accurately the migration of single solitary wave. Then, the interaction of two and three solitary waves and evolution of solitons are studied. A linear stability analysis based on the Fourier method is also investigated.

2 The Governing Equation and Cubic B-Splines

In this study, we will consider the modified Korteweg-de Vries (mKdV) equation

$$U_t + \varepsilon U^2 U_x + \mu U_{xxx} = 0, \tag{1}$$

with the physical boundary conditions $U \to 0$ as $x \to \pm\infty$, where ε and μ are positive parameters and the subscripts x and t denote the differentiation. In Eq. (1), the derivative U_t characterizes the time evolution of the wave propagating in one direction, the nonlinear term U^2U_x describes the steepening of the wave, and the linear term U_{xxx} stands for the spreading or dispersion of the wave.

To implement the numerical method, solution domain is restricted over an interval $a \le x \le b$. Boundary conditions will be selected from the following homogeneous boundary conditions:

$$\begin{aligned} &U(a,t) = 0, \qquad U(b,t) = 0, \\ &U_x(a,t) = 0, \qquad U_x(b,t) = 0, \qquad t > 0, \end{aligned} \tag{2}$$

and the initial condition

$$U(x,0) = f(x), \quad a \le x \le b. \tag{3}$$

The cubic B-splines $\phi_m(x)$ for $m = -1(1)N+1$, at the knots x_m are defined over the interval $[a, b]$ by the relationships (Prenter 1975):

$$\phi_m(x) = \frac{1}{h^3}\begin{cases} (x - x_{m-2})^3, & x \in [x_{m-2}, x_{m-1}], \\ h^3 + 3h^2(x - x_{m-1}) + 3h(x - x_{m-1})^2 - 3(x - x_{m-1})^3, & x \in [x_{m-1}, x_m], \\ h^3 + 3h^2(x_{m+1} - x) + 3h(x_{m+1} - x)^2 - 3(x_{m+1} - x)^3, & x \in [x_m, x_{m+1}], \\ (x_{m+2} - x)^3, & x \in [x_{m+1}, x_{m+2}], \\ 0, & \text{otherwise}. \end{cases} \tag{4}$$

The set of functions $\{\phi_{-1}(x), \phi_0(x), \ldots, \phi_{N+1}(x)\}$ forms a basis for approximate solution defined over $[a, b]$. The approximate solution $U_N(x,t)$ to the exact solution $U(x, t)$ is given by

$$U_N(x,t) = \sum_{j=-1}^{N+1} \phi_j(x)\delta_j(t), \tag{5}$$

where $\delta_j(t)$ are time-dependent parameters to be determined from the boundary and weighted residual conditions. Each cubic B-spline covers four elements so that each element $[x_m, x_{m+1}]$ is covered by four splines. In each element, using the following local coordinate transformation:

$$h\xi = x - x_m, \quad 0 \le \xi \le 1, \tag{6}$$

cubic B-spline shape functions in terms of ξ over the domain $[x_{m-1}, x_{m+2}]$ can be defined as

$$\begin{matrix} \phi_{m-1} \\ \phi_m \\ \phi_{m+1} \\ \phi_{m+2} \end{matrix} = \begin{cases} (1-\xi)^3, \\ 1 + 3(1-\xi) + 3(1-\xi)^2 - 3(1-\xi)^3, \\ 1 + 3\xi + 3\xi^2 - 3\xi^3, \\ \xi^3. \end{cases} \tag{7}$$

All splines apart from $\phi_{m-1}(x), \phi_m(x), \phi_{m+1}(x)$ and $\phi_{m+2}(x)$ are zero over the element $[x_m, x_{m+1}]$. Variation of the function $U(x, t)$ over element $[x_m, x_{m+1}]$ is approximated by

$$U_N(\xi,t) = \sum_{j=m-1}^{m+2} \delta_j\phi_j, \tag{8}$$

Table 1 Cubic B-splines and its derivatives at nodes x_m

x	x_{m-2}	x_{m-1}	x_m	x_{m+1}	x_{m+2}
$\phi_m(x)$	0	1	4	1	0
$h\phi'_m(x)$	0	3	0	-3	0
$h^2\phi''_m(x)$	0	6	-12	6	0

where $\delta_{m-1}, \delta_m, \delta_{m+1}, \delta_{m+2}$ act as element parameters and B-splines $\phi_{m-1}, \phi_m, \phi_{m+1}, \phi_{m+2}$ as element shape functions. The values of $\phi_m(x)$ and its derivatives may be tabulated as in Table 1.

Using trial function (5) and cubic splines (4), the values of U, U', U'' at the knots are determined in terms of the element parameters δ_m by

$$\begin{aligned} U_m &= U(x_m) = \delta_{m-1} + 4\delta_m + \delta_{m+1}, \\ hU'_m &= U'(x_m) = 3(-\delta_{m-1} + \delta_{m+1}), \\ h^2U''_m &= U''(x_m) = 6(\delta_{m-1} - 2\delta_m + \delta_{m+1}), \end{aligned} \tag{9}$$

where the symbols $'$ and $''$ denotes first and second differentiation with respect to x, respectively. The splines $\phi_m(x)$ and its two principle derivatives vanish outside the interval $[x_{m-2}, x_{m+2}]$.

3 Galerkin Finite Element Method

By applying the Galerkin method to Eq. (1) with weight function $W(x)$, the weak form of Eq. (1) is obtained as

$$\int_a^b W(U_t + \varepsilon U^2 U_x + \mu U_{xxx})\mathrm{d}x = 0. \tag{10}$$

For a single element $[x_m, x_{m+1}]$, using transformation (6) into the Eq. (10) and

$$\int_0^1 W\left[U_t + \varepsilon\left(\frac{U^2}{h}\right)U_\xi + \mu\left(\frac{1}{h^3}\right)U_{\xi\xi\xi}\right]\mathrm{d}\xi = 0, \tag{11}$$

integrating Eq. (11) by parts and using Eq. (1) lead to

$$\int_0^1 [W(U_t + \varepsilon\lambda U_\xi) - (\eta W_\xi U_{\xi\xi})]\mathrm{d}\xi + \eta W U_{\xi\xi}|_0^1 = 0, \tag{12}$$

where $\lambda = \frac{U^2}{h}$ and $\eta = \frac{\mu}{h^3}$. Taking the weight function as cubic B-spline shape functions given by Eq. (7) and substituting approximation (8) in integral equation (12) with some manipulation, we obtain the element contributions in the form:

$$\sum_{j=m-1}^{m+2}\left[\int_0^1 \phi_i\phi_j \mathrm{d}\xi\right]\dot{\delta}_j^e + \sum_{j=m-1}^{m+2}\left[\left(\varepsilon\lambda\int_0^1 \phi_i\phi'_j\mathrm{d}\xi\right) - \left(\eta\int_0^1 \phi'_i\phi''_j\mathrm{d}\xi\right) + \left(\eta\phi_i\phi''_j|_0^1\right)\right]\delta_j^e = 0. \tag{13}$$

In matrix notation, this equation becomes

$$[A^e]\dot{\delta}^e + [\varepsilon\lambda B^e - \eta(C^e - D^e)]\delta^e = 0, \tag{14}$$

where $\delta^e = (\delta_{m-1}, \delta_m, \delta_{m+1}, \delta_{m+2})^T$ are the element parameters and the dot denotes differentiation with respect to t. The element matrices A^e, B^e, C^e and D^e are given by the following integrals:

$$A^e_{ij} = \int_0^1 \phi_i\phi_j\mathrm{d}\xi = \frac{1}{140}\begin{bmatrix} 20 & 129 & 60 & 1 \\ 129 & 1188 & 933 & 60 \\ 60 & 933 & 1188 & 129 \\ 1 & 60 & 129 & 20 \end{bmatrix}$$

$$B^e_{ij} = \int_0^1 \phi_i\phi'_j\mathrm{d}\xi = \frac{1}{20}\begin{bmatrix} -10 & -9 & 18 & 1 \\ -71 & -150 & 183 & 38 \\ -38 & -183 & 150 & 71 \\ -1 & -18 & 9 & 10 \end{bmatrix}$$

$$C^e_{ij} = \int_0^1 \phi'_i\phi''_j\mathrm{d}\xi = \frac{1}{2}\begin{bmatrix} -9 & 15 & -3 & -3 \\ -15 & 9 & 27 & -21 \\ 21 & -27 & -9 & 15 \\ 3 & 3 & -15 & 9 \end{bmatrix}$$

$$D^e_{ij} = \phi_i\phi''_j|_0^1 = \begin{bmatrix} -6 & 12 & -6 & 0 \\ -24 & 54 & -36 & 6 \\ -6 & 36 & -54 & 24 \\ 0 & 6 & -12 & 6 \end{bmatrix}$$

where the suffices i, j take only the values $m-1, m, m+1, m+2$ for the typical element $[x_m, x_{m+1}]$. A lumped value for λ is found from $(U_m + U_{m+1})^2/4$ as

$$\lambda = \frac{1}{4h}(\delta_{m-1} + 5\delta_m + 5\delta_{m+1} + \delta_{m+2})^2. \tag{15}$$

By assembling all contributions from all elements, Eq. (14) leads to the following matrix equation:

$$[A]\dot{\delta} + [\varepsilon\lambda B - \eta(C - D)]\delta = 0, \tag{16}$$

where $\delta = (\delta_{-1}, \delta_0 \ldots \delta_N, \delta_{N+1})^T$ are global element parameters. The matrices $A, \lambda B, C$ and D are septadiagonal and row of each has the following form:

$$\begin{aligned} A &= \frac{1}{140}(1, 120, 1191, 2416, 1191, 120, 1), \\ \lambda B &= \frac{1}{20}(-\lambda_1, -18\lambda_1 - 38\lambda_2, 9\lambda_1 - 183\lambda_2 \\ &\quad -71\lambda_3, 10\lambda_1 + 150\lambda_2 - 150\lambda_3 - 10\lambda_4, \\ &\quad 71\lambda_2 + 183\lambda_3 - 9\lambda_4, 38\lambda_3 + 18\lambda_4, \lambda_4), \\ C &= \frac{1}{2}(3, 24, -57, 0, 57, -24, -3), \\ D &= (0, 0, 0, 0, 0, 0, 0), \end{aligned}$$

where

$$\lambda_1=\frac{1}{4h}(\delta_{m-2}+5\delta_{m-1}+5\delta_m+\delta_{m+1})^2,$$
$$\lambda_2=\frac{1}{4h}(\delta_{m-1}+5\delta_m+5\delta_{m+1}+\delta_{m+2})^2,$$
$$\lambda_3=\frac{1}{4h}(\delta_m+5\delta_{m+1}+5\delta_{m+2}+\delta_{m+3})^2,$$
$$\lambda_4=\frac{1}{4h}(\delta_{m+1}+5\delta_{m+2}+5\delta_{m+3}+\delta_{m+4})^2.$$

Replacing the time derivative of the parameter $\dot{\delta}$ by usual forward finite-difference approximation and parameter δ by the Crank–Nicolson formulation:

$$\dot{\delta}=\frac{1}{\Delta t}\left(\delta^{n+1}-\delta^n\right),\ \delta=\frac{1}{2}\left(\delta^{n+1}+\delta^n\right) \tag{17}$$

into Eq. (16), it gives the $(N+3)\times(N+3)$ septadiagonal matrix system:

$$\begin{aligned}&\left\{A+[\varepsilon\lambda B-\eta(C-D)]\frac{\Delta t}{2}\right\}\delta^{n+1}\\ &\quad=\left\{A-[\varepsilon\lambda B-\eta(C-D)]\frac{\Delta t}{2}\right\}\delta^n\end{aligned} \tag{18}$$

where Δt is time step. Applying the boundary conditions (2) to the system (18), we obtain a $(N+1)\times(N+1)$ septadiagonal matrix system. This system is efficiently solved with a variant of the Thomas algorithm, but an inner iteration is also needed at each time step to cope with the nonlinear term. A typical member of the matrix system (18) may be written in terms of the nodal parameters δ^n and δ^{n+1} as

$$\begin{aligned}&\gamma_1\delta^{n+1}_{m-3}+\gamma_2\delta^{n+1}_{m-2}+\gamma_3\delta^{n+1}_{m-1}+\gamma_4\delta^{n+1}_{m}+\gamma_5\delta^{n+1}_{m+1}\\ &\quad+\gamma_6\delta^{n+1}_{m+2}+\gamma_7\delta^{n+1}_{m+3}\\ &\quad=\gamma_7\delta^{n}_{m-3}+\gamma_6\delta^{n}_{m-2}+\gamma_5\delta^{n}_{m-1}+\gamma_4\delta^{n}_{m}+\gamma_3\delta^{n}_{m+1}\\ &\quad+\gamma_2\delta^{n}_{m+2}+\gamma_1\delta^{n}_{m+3}\end{aligned} \tag{19}$$

where

$$\gamma_1=\frac{1}{140}-\frac{\varepsilon\lambda\Delta t}{240}-\frac{3\eta\Delta t}{4},$$
$$\gamma_2=\frac{120}{140}-\frac{56\varepsilon\lambda\Delta t}{240}-\frac{24}{4}\eta\Delta t,$$
$$\gamma_3=\frac{1191}{140}-\frac{245\varepsilon\lambda\Delta t}{240}+\frac{57\eta\Delta t}{4},$$
$$\gamma_4=\frac{2416}{140},$$
$$\gamma_5=\frac{1191}{140}+\frac{245\varepsilon\lambda\Delta t}{240}-\frac{57\eta\Delta t}{4},$$
$$\gamma_6=\frac{120}{140}+\frac{56\varepsilon\lambda\Delta t}{240}+\frac{24}{4}\eta\Delta t,$$
$$\gamma_7=\frac{1}{140}+\frac{\varepsilon\lambda\Delta t}{240}+\frac{3\eta\Delta t}{4},$$

which all depend on δ^n. The initial vector of parameters $\delta^0=(\delta^0_{-1},\ldots,\delta^0_{N+1})$ must be determined to iterate the system (18). To do this, the approximation is rewritten over the interval $[a,b]$ at time $t=0$ as follows:

$$U_N(x,0)=\sum_{m=-1}^{N+1}\phi_m(x)\delta^0_m \tag{20}$$

where the parameters δ^0_m will be determined. $U_N(x,0)$ are required to satisfy the following relations at the mesh points x_m:

$$\begin{aligned}&U_N(x_m,0)=U(x_m,0),m=0,1,\ldots,N.\\ &\quad U'_N(x_0,0)=U'(x_N,0)=0.\end{aligned} \tag{21}$$

The above conditions lead to a tridiagonal matrix system of the form

$$\begin{bmatrix}-3&0&3&&&\\1&4&1&&&\\&&&\ddots&&\\&&&1&4&1\\&&&-3&0&3\end{bmatrix}\begin{bmatrix}\delta^0_{-1}\\ \delta^0_0\\ \vdots\\ \delta^0_N\\ \delta^0_{N+1}\end{bmatrix}=\begin{bmatrix}U'(x_0,0)\\U(x_0,0)\\ \vdots\\ U(x_N,0)\\U'(x_N,0)\end{bmatrix}$$

which can be solved using a variant of the Thomas algorithm.

3.1 The Solution of Septadiagonal Matrix System with Thomas Algorithm

The solution method of septadiagonal matrix system with Thomas algorithm is stated as the following (Zeybek and Karakoc 2016). The system can be written by

$$\begin{aligned}&a_i\delta_{i-3}+b_i\delta_{i-2}+c_i\delta_{i-1}+d_i\delta_i+e_i\delta_{i+1}+f_i\delta_{i+2}+g_i\delta_{i+3},\\ &\quad i=0,1,\ldots,N\end{aligned} \tag{22}$$

and

$$\begin{aligned}&a_0=b_0=c_0=a_1=b_1=a_2=g_{N-2}=g_{N-1}=f_{N-1}\\ &\quad=g_N=f_N=e_N=0.\end{aligned} \tag{23}$$

First, the parameters are taken as

$$\begin{aligned}&\alpha_0=b_0,\ \beta_0=c_0,\ \mu_0=d_0,\ \zeta_0=\frac{e_0}{\mu_0},\ \lambda_0=\frac{f_0}{\mu_0},\ \eta_0=\frac{g_0}{\mu_0},\ \gamma_0=\frac{h_0}{\mu_0},\\ &\alpha_1=b_1,\ \beta_1=c_1,\ \mu_1=d_1-\beta_1\zeta_0,\\ &\zeta_1=\frac{e_1-\beta_1\lambda_0}{\mu_1},\ \lambda_1=\frac{f_1-\beta_1\gamma_0}{\mu_1},\ \eta_1=\frac{g_1}{\mu_1},\ \gamma_1=\frac{h_1-\beta_1\gamma_0}{\mu_1},\end{aligned} \tag{24}$$

and

$$\alpha_2 = b_2,\ \beta_2 = c_2 - \alpha_2\zeta_0,\ \mu_2 = d_2 - \lambda_0\alpha_2 - \beta_2\zeta_1,\quad \zeta_2 = \frac{e_2 - \eta_0\alpha_2 - \beta_2\lambda_1}{\mu_2},\ \lambda_2 = \frac{f_2 - \beta_2\eta_1}{\mu_2},\quad \eta_2 = \frac{g_2}{\mu_2},\ \gamma_2 = \frac{h_2 - \alpha_2\gamma_0 - \beta_2\gamma_1}{\mu_2}. \tag{25}$$

Second, the following parameters are computed for $i = 0, 1, \ldots, N$:

$$\begin{aligned} \alpha_i &= b_i - a_i\zeta_{i-3},\\ \beta_i &= c_i - a_i\lambda_{i-3} - \alpha_i\zeta_{i-2},\\ \mu_i &= d_i - a_0\eta_{i-3} - \lambda_{i-2}\alpha_i - \beta_i\zeta_{i-1},\\ \zeta_i &= \frac{e_i - \eta_{i-2}\alpha_i - \beta_i\lambda_{i-1}}{\mu_i},\\ \lambda_i &= \frac{f_i - \beta_i\eta_{i-1}}{\mu_i},\\ \eta_i &= \frac{g_i}{\mu_i},\\ \gamma_i &= \frac{h_i - \beta_i\gamma_{i-1} - \alpha_i\gamma_{i-2} - a_i\gamma_{i-3}}{\mu_i}. \end{aligned} \tag{26}$$

Then, the solution is given by

$$\delta_{N-2} = \gamma_{N-2} - \lambda_{N-2}\delta_N - \eta_{N-2}\delta_{N-1},\ \delta_{N-1} = \gamma_{N-1} - \eta_{N-1}\delta_N,\ \delta_N = \gamma_N \tag{27}$$

and

$$\delta_i = \gamma_i - \zeta_i\delta_{i+1} - \lambda_i\delta_{i+2} - \eta_i\delta_{i+3},\ i = 0, 1, \ldots, \mathrm{N}-4, \mathrm{N}-3. \tag{28}$$

4 Stability Analysis

The stability analysis is based on the von Neumann theory. The growth factor ξ of the error in a typical mode of amplitude:

$$\delta_m^n = \xi^n e^{ijkh}, \tag{29}$$

where k is the mode number and h is the element size, and is determined from a linearization of the numerical scheme. To apply the stability analysis, the mKdV equation can be linearized by assuming that the quantity U^2 in the nonlinear term U^2U_x is locally constant. Substituting the Fourier mode (29) into (19), it gives the growth factor ξ of the form:

$$\xi = \frac{a - ib}{a + ib}, \tag{30}$$

where

$$\begin{aligned} a =& 14496 + 8292\cos(kh) + 1440\cos(2kh) + 12\cos(3kh),\\ b =& -[6000 - (1715\varepsilon\lambda - 23940\eta)\Delta t]\sin(kh)\\ &+ [(392\varepsilon\lambda + 10080\eta)\Delta t]\sin(2kh)\\ &+ [(7\varepsilon\lambda + 1260\eta)\Delta t]\sin(3kh). \end{aligned} \tag{31}$$

The modulus of $|\xi|$ is 1; therefore, the linearized scheme is unconditionally stable.

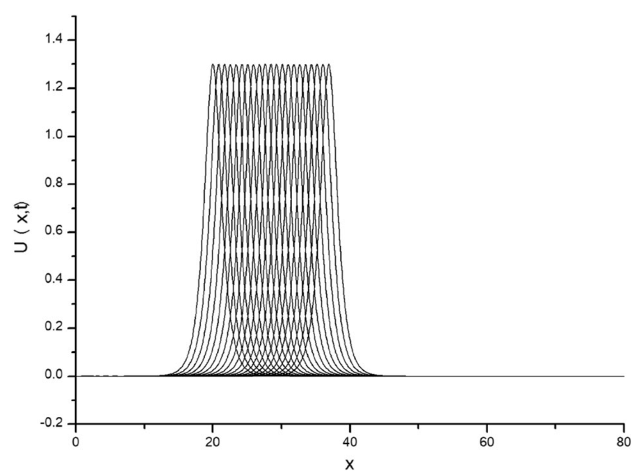

Fig. 1 Single solitary wave with $\varepsilon = 3$, $\mu = 1$, $c = 0.845$, $h = 0.1$, $\Delta t = 0.01$ and $0 \le x \le 80$ at $t = 0, 1, 2, \ldots, 20$

Table 2 Invariants and error norms for single solitary wave with $\varepsilon = 3$, $\mu = 1$, $c = 0.845$, $h = 0.1$ and $\Delta t = 0.01$, $0 \le x \le 80$

t		1	5	10	15	20
I_1	Present (Biswas and Raslan 2011)	4.442866	4.442866	4.442866	4.442866	4.442866
		4.443000	4.443138	4.444142	4.443420	4.443171
I_2	Present (Biswas and Raslan 2011)	3.676941	3.676941	3.676941	3.676941	3.676941
		3.677069	3.677535	3.678094	3.678642	3.679192
I_3	Present (Biswas and Raslan 2011)	2.072792	2.073533	2.073695	2.073772	2.073841
		2.073575	2.074357	2.075303	2.076232	2.077161
L_2-Error	Present (Biswas and Raslan 2011)	6.279015e−04	1.252048e−03	2.138787e−03	2.960441e−03	3.656694e−03
		–	–	–	–	–
L_∞-Error	Present (Biswas and Raslan 2011)	3.624348e−04	8.415234e−04	1.403498e−03	1.887116e−03	2.294197e−03
		1.206756e−03	3.621519e−03	5.942047e−03	7.626772e−03	8.642137e−03

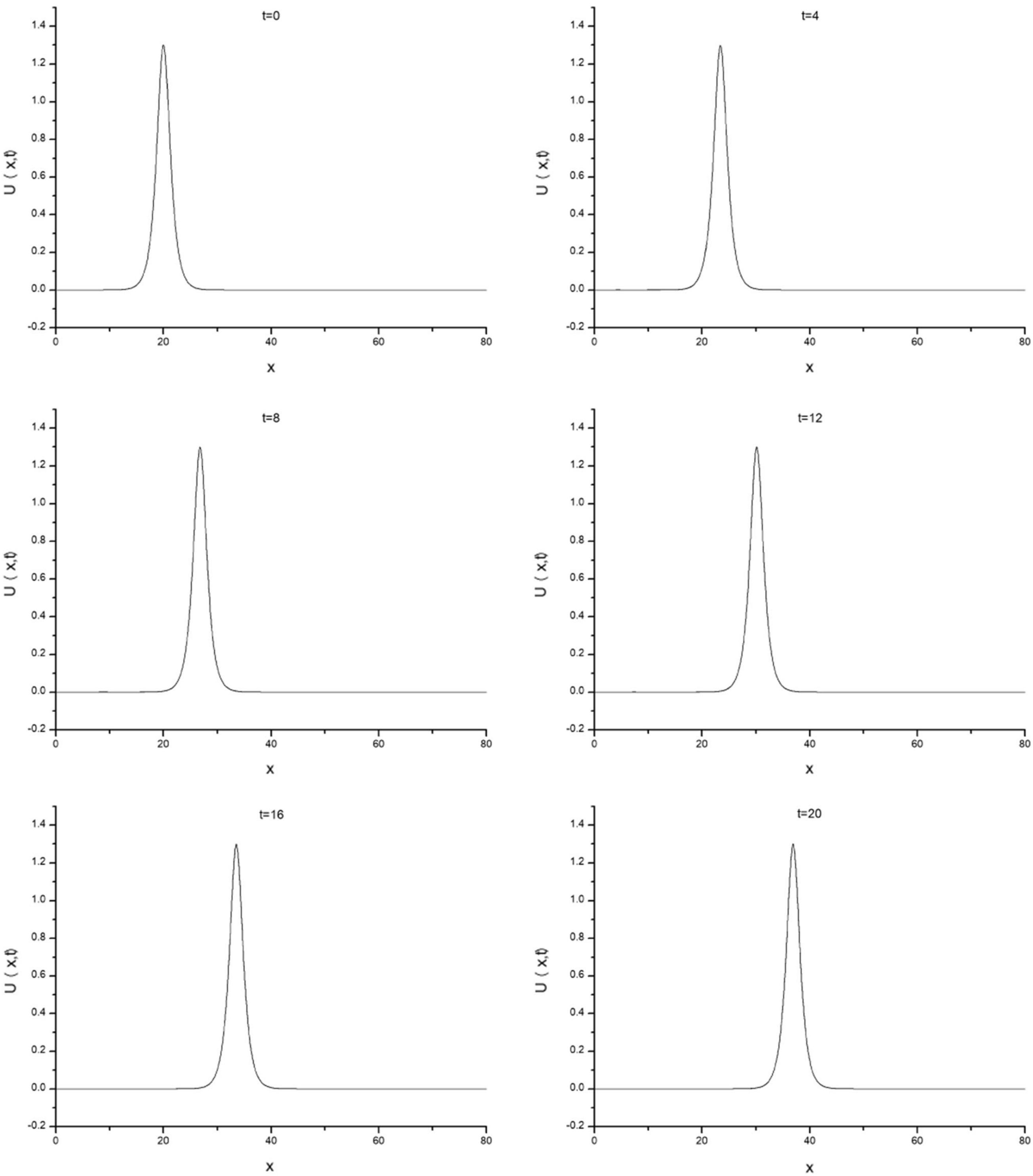

Fig. 2 Single solitary wave with $\varepsilon = 3$, $\mu = 1$, $c = 0.845$, $h = 0.1$, $\Delta t = 0.01$ and $0 \le x \le 80$ at $t = 0, 4, 8, 12, 16$ and 20

5 Numerical Examples and Results

Numerical results of the mKdV equation are obtained for three problems: the motion of single solitary wave, interaction of two and three solitary waves. We use

$$L_2 = \|U^{\text{exact}} - U_N\|_2 \simeq \sqrt{h\sum_{j=1}^{N}\left|U_j^{\text{exact}} - (U_N)_j\right|^2}, \qquad (32)$$

the error norm L_2

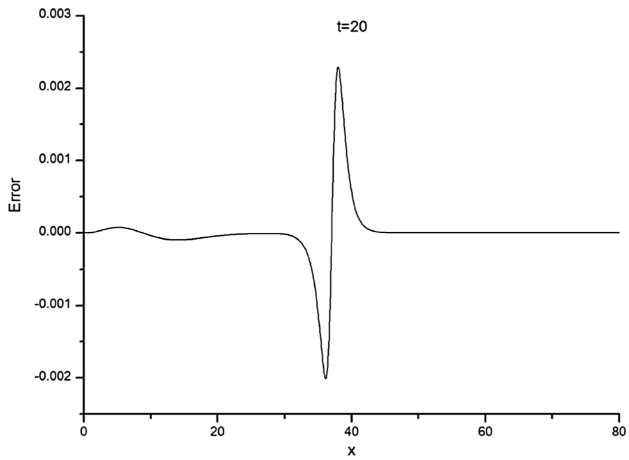

Fig. 3 Error with $\varepsilon = 3$, $\mu = 1$, $c = 0.845$, $h = 0.1$ and $\Delta t = 0.01, 0 \leq x \leq 80$, $t = 20$

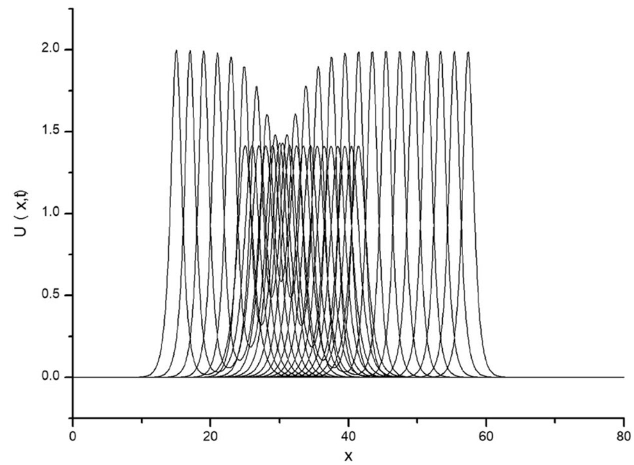

Fig. 4 Interaction of two solitary waves with $\varepsilon = 3$, $\mu = 1$, $h = 0.1$, $\Delta t = 0.01$, $c_1 = 2$, $c_2 = 1$, $x_1 = 15$, $x_2 = 25$ and $0 \leq x \leq 80$ at $t = 0, 1, 2, \ldots, 20$

$$L_\infty = \|U^{\text{exact}} - U_N\|_\infty \simeq \max_j \left| U_j^{\text{exact}} - (U_N)_j \right|, j = 1, 2, \ldots, N, \tag{33}$$

and the error norm L_∞ to calculate the difference between analytical and numerical solutions at some specified times. mKdV equation (1) possesses only three conservation constants given by

$$\begin{aligned} I_1 &= \int_a^b U \mathrm{d}x \simeq h \sum_{j=1}^{N} U_j^n, \\ I_2 &= \int_a^b U^2 \mathrm{d}x \simeq h \sum_{j=1}^{N} (U_j^n)^2, \\ I_3 &= \int_a^b \left[U^4 - \frac{6\mu}{\varepsilon} (U_x)^2 \right] \mathrm{d}x \simeq h \sum_{j=1}^{N} \left[(U_j^n)^4 - \frac{6\mu}{\varepsilon} (U_x)_j^n \right], \end{aligned} \tag{34}$$

which correspond to conversation of mass, momentum, and energy, respectively (Miura et al. 1968; Miura 1976). In the simulation of solitary wave motion, the invariants I_1, I_2, and I_3 are monitored to check the accuracy of the numerical algorithm.

5.1 The Motion of Single Solitary Wave

The solitary wave solution of the mKdV equation (1) is considered with the boundary conditions $U \to 0$ as $x \to \pm\infty$ and the initial condition:

$$U(x,t) = \sqrt{\frac{6c}{\varepsilon}} \operatorname{sech} \left[\sqrt{\frac{c}{\mu}} (x - ct - x_0) \right], \tag{35}$$

where ε, μ, c, and x_0 are arbitrary constants. The initial condition is

$$U(x,0) = \sqrt{\frac{6c}{\varepsilon}} \operatorname{sech} \left[\sqrt{\frac{c}{\mu}} (x - x_0) \right]. \tag{36}$$

The conserved quantities of motion for a solitary wave of amplitude $\sqrt{\frac{6c}{\varepsilon}}$ and width depending on $\sqrt{\frac{c}{\mu}}$ may be evaluated analytically as (Biswas and Raslan 2011)

$$I_1 = \pi \sqrt{\frac{6\mu}{\varepsilon}}, \quad I_2 = \frac{12\sqrt{\mu c}}{\varepsilon}, \quad I_3 = -\frac{64c^2}{\varepsilon^2} \sqrt{\frac{\mu}{c}}. \tag{37}$$

For the numerical simulation of the motion of a single solitary wave, parameters $\varepsilon = 3$, $\mu = 1$, $c = 0.845$, $h = 0.1$ and $\Delta t = 0.01$ over the interval $[0, 80]$ are chosen to coincide with another study (Biswas and Raslan 2011). For these parameters, the solitary wave has an amplitude 1.3. The conserved quantities and error norms L_2 and L_∞ are shown at selected times up to time $t = 20$. The obtained results are tabulated in Table 2. It can be seen from Table 2 that the error norms L_2 and L_∞ are found to be small

Table 3 Comparison of invariants for the interaction of two solitary waves with $\varepsilon = 3$, $\mu = 1$, $h = 0.1$, $\Delta t = 0.01$, $c_1 = 2$, $c_2 = 1$, $x_1 = 15$ and $x_2 = 25$, $0 \leq x \leq 80$

	t	1	5	10	15	20
I_1	Present (Biswas and Raslan 2011)	8.885732	8.885732	8.885732	8.885732	8.885732
		8.886014	8.886776	8.889742	8.885983	8.884880
I_2	Present (Biswas and Raslan 2011)	9.659345	9.659345	9.659345	9.659345	9.659345
		9.659527	9.663714	9.662547	9.661071	9.661224
I_3	Present (Biswas and Raslan 2011)	10.270822	10.857214	10.954278	10.307099	10.338321
		10.239870	10.249000	10.246790	10.242580	10.242030

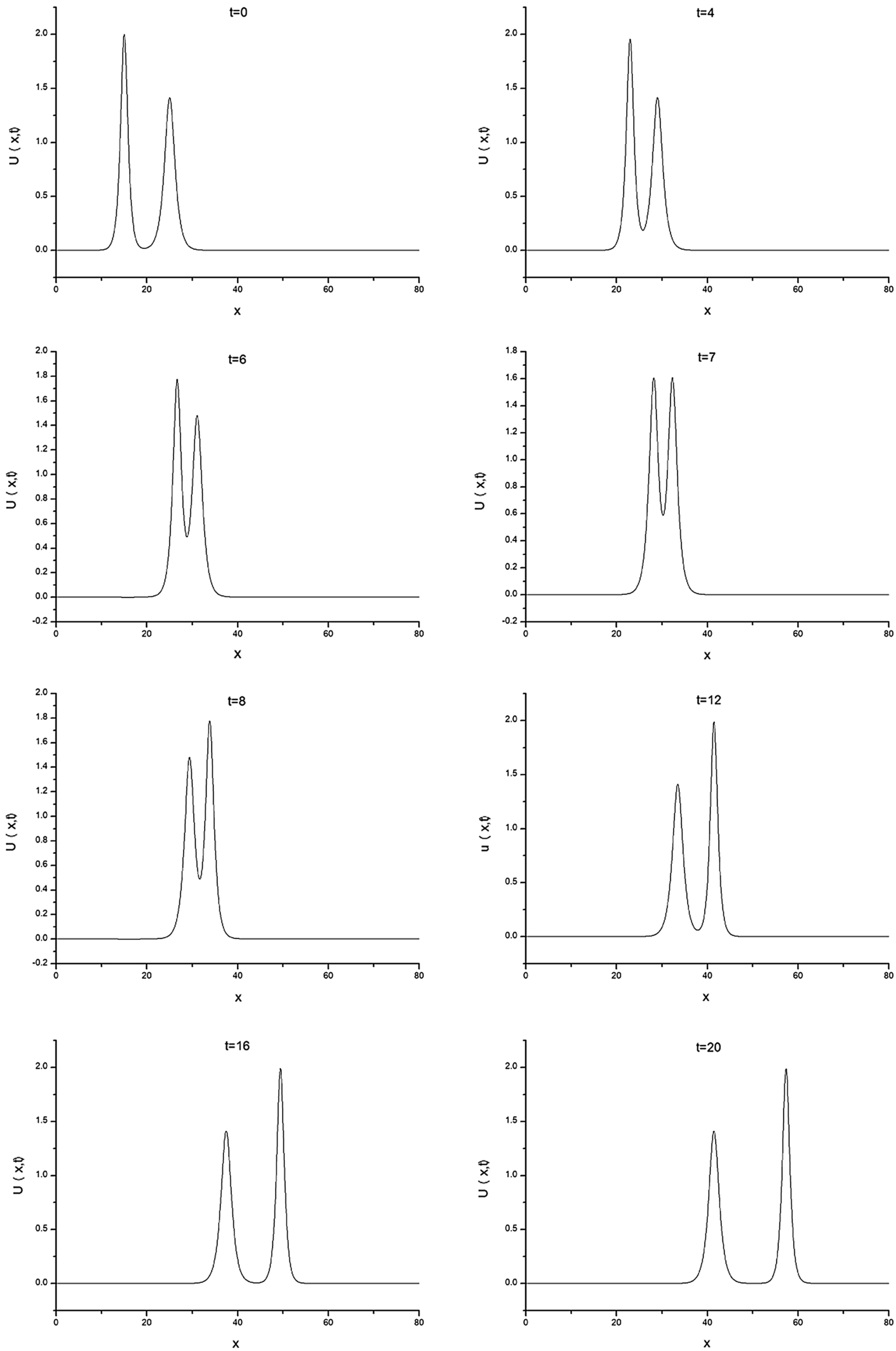
t=0
t=4
t=6
t=7
t=8
t=12
t=16
t=20
U (x,t)
u (x,t)
x

◀**Fig. 5** Interaction of two solitary waves with $\varepsilon = 3$, $\mu = 1$, $h = 0.1$, $\Delta t = 0.01$, $c_1 = 2$, $c_2 = 1$, $x_1 = 15$, $x_2 = 25$ and $0 \le x \le 80$ at $t = 0, 4, 6, 7, 8, 12, 16$ and 20

enough and the quantities in the invariants remain almost constant during the computer run. Table 2 represents a comparison of the values of the invariants and error norms obtained by the present method with those obtained in Biswas and Raslan (2011). It is clearly observed from the Table 2 that the error norms obtained by the present method are smaller than another method (Biswas and Raslan 2011). In Fig. 1, the numerical solutions are displayed at $t = 0, 1, 2, \ldots, 20$. For numerical solution of single solitary wave, the graphs are plotted with $\varepsilon = 3$, $\mu = 1$, $c = 0.845$, $h = 0.1$ and $\Delta t = 0.01$ at selected times from $t = 0$ to $t = 20$, in Fig. 2. To show the errors between the analytical and numerical results over the problem domain, errors' distributions are depicted for solitary waves with amplitudes 1.3 at time $t = 20$ in Fig. 3.

5.2 Interaction of Two Solitary Waves

In this problem, we consider the interaction of two solitary waves using the initial condition given by the linear sum of two well-separated solitary waves having various amplitudes:

$$U(x,0) = \sum_{i=1}^{2} \alpha_i \operatorname{sech}\left[\beta_i (x - x_i)\right], \tag{38}$$

where $\alpha_i = \sqrt{\frac{6c_i}{\varepsilon}}$, $\beta_i = \sqrt{\frac{c_i}{\mu}}$, c_i, and x_i are arbitrary constants for $i = 1, 2$.

For the simulation, the parameters $\varepsilon = 3$, $\mu = 1$, $h = 0.1$, $\Delta t = 0.01$, $c_1 = 2$, $c_2 = 1$, $x_1 = 15$ and $x_2 = 25$ are chosen over the range $0 \le x \le 80$ to coincide with those used by Biswas and Raslan (2011). The experiment are run from $t = 0$ to $t = 20$ and the calculated values of the invariants I_1, I_2 and I_3 obtained by the present method with those obtained in Biswas and Raslan (2011) are compared in Table 3. It is seen that the obtained values of the invariants remain almost constant during the computer run.

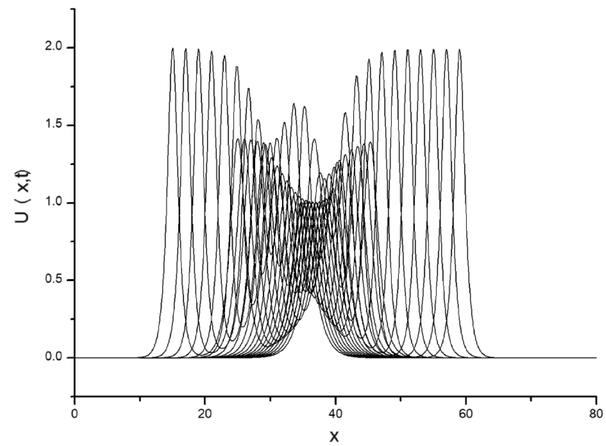

Fig. 6 Interaction of three solitary waves with $\varepsilon = 3$, $\mu = 1$, $h = 0.1$, $\Delta t = 0.01$, $c_1 = 2$, $c_2 = 1$, $c_3 = 0.5$, $x_1 = 15$, $x_2 = 25$ and $x_3 = 35$ and $0 \le x \le 80$ at $t = 0, 1, 2, \ldots, 20$

The interaction of two solitary waves scenarios is showed at $t = 0, 1, 2, \ldots, 20$ in Fig. 4.

Figure 5 shows the development of the interaction of two solitary waves. It is clear from the figure that, at $t = 0$, the greater soliton is at the left position of the smaller soliton, at the beginning of the run. With the increases of the time, the greater soliton catches up the smaller until at time $t = 7$, then the smaller soliton is absorbed. The overlapping process continues until $t = 8$, and the greater soliton has overtaken the smaller soliton and get in the process of the separating. At time $t = 16$, the interaction is completed and the greater soliton has separated completely.

5.3 Interaction of Three Solitary Waves

As a last problem, we study the behavior of the interaction of three solitary waves having different amplitudes and traveling in the same direction. Therefore, we consider Eq. (1) with initial condition given by the linear sum of three well-separated solitary waves of different amplitudes:

$$U(x,0) = \sum_{i=1}^{3} \alpha_i \operatorname{sech}\left[\beta_i (x - x_i)\right], \tag{39}$$

Table 4 Comparison of invariants for the interaction of three solitary waves with $\varepsilon = 3$, $\mu = 1$, $h = 0.1$, $\Delta t = 0.01$, $c_1 = 2$, $c_2 = 1$, $c_3 = 0.5$, $x_1 = 15$, $x_2 = 25$ and $x_3 = 35$, $0 \le x \le 80$

	t	1	5	10	15	20
I_1	Present (Biswas and Raslan 2011)	13.328677	13.328677	13.328677	13.328677	13.328677
		13.329060	13.330630	13.338780	13.332640	13.332060
I_2	Present (Biswas and Raslan 2011)	12.519943	12.519943	12.519943	12.519943	12.519943
		12.520280	12.526260	12.540860	12.526660	12.524900
I_3	Present (Biswas and Raslan 2011)	11.321178	13.483073	12.415348	12.413743	11.499146
		11.249790	11.261270	11.288040	11.259970	11.256730

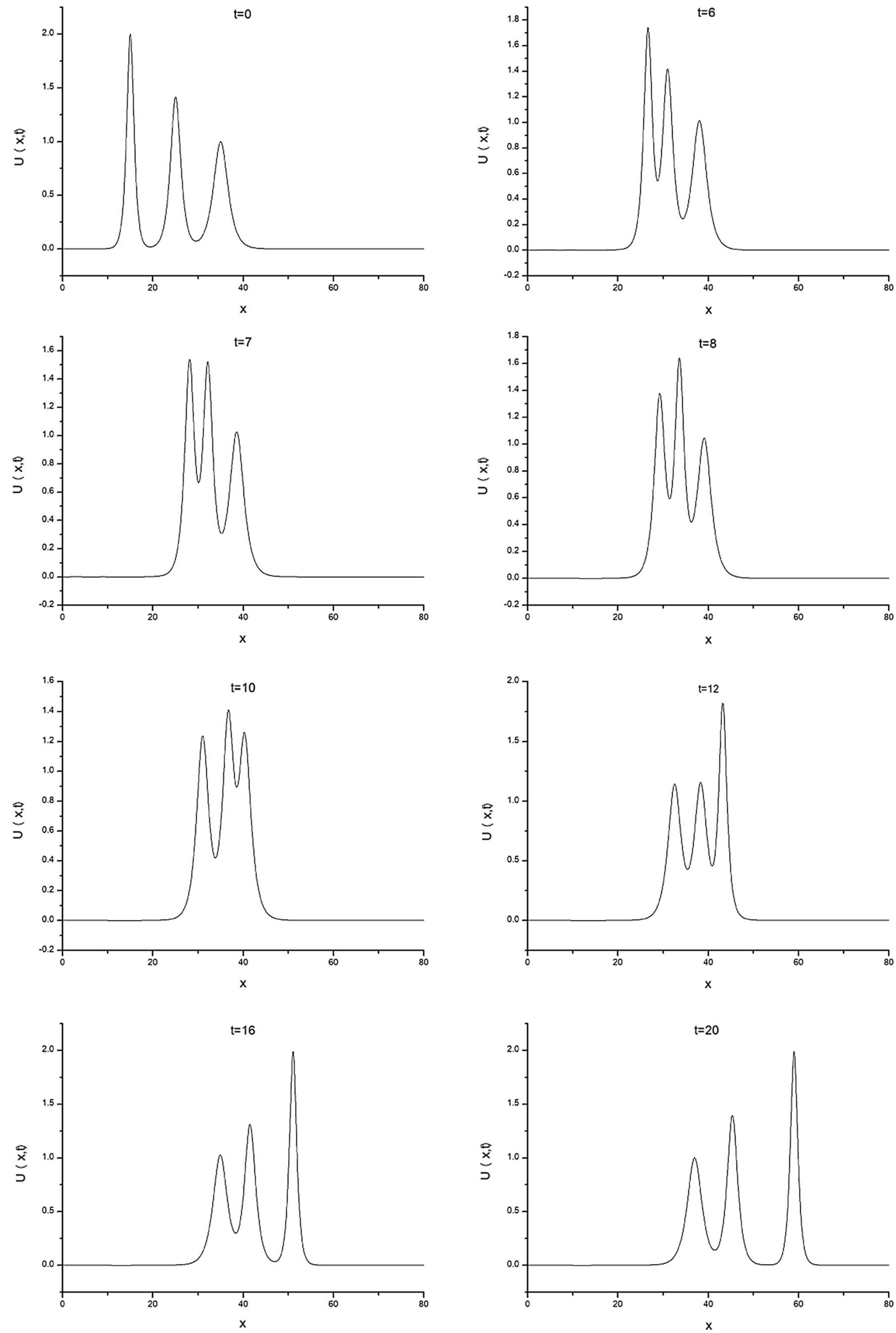
t=0
t=6
t=7
t=8
t=10
t=12
t=16
t=20
U (x,t)
x

◀**Fig. 7** Interaction of three solitary waves with $\varepsilon = 3$, $\mu = 1$, $h = 0.1$, $\Delta t = 0.01$, $c_1 = 2$, $c_2 = 1$, $c_3 = 0.5$, $x_1 = 15$, $x_2 = 25$, $x_3 = 35$ and $0 \le x \le 80$ at $t = 0, 6, 7, 8, 10, 12, 16$ and 20

where $\alpha_i = \sqrt{\frac{6c_i}{\varepsilon}}$, $\beta_i = \sqrt{\frac{c_i}{\mu}}$, c_i, and x_i are arbitrary constants for $i = 1, 2, 3$.

For the computational work, parameters $\varepsilon = 3$, $\mu = 1$, $h = 0.1$, $\Delta t = 0.01$, $c_1 = 2$, $c_2 = 1$, $c_3 = 0.5$, $x_1 = 15$, $x_2 = 25$, and $x_3 = 35$ are taken over the interval $0 \le x \le 80$. Simulations are done up to time $t = 20$. Table 4 displays a comparison of the values of the invariants obtained by the present method with those obtained in Biswas and Raslan (2011). It is seen from the table that the obtained values of the invariants remain almost constant during the computer run. Figure 6 shows the interaction of these solitary waves at $t = 0, 1, 2, \ldots, 20$. As it is seen from Fig. 7, interaction started about time $t = 6$, overlapping processes occured

Table 5 Invariants for Gaussian initial condition with $\mu = 0.1$ and $\mu = 0.04$, $h = 0.1$, $\Delta t = 0.01$ and $-50 \le x \le 50$ at $0 \le t \le 10$

t	$\mu = 0.1$			$\mu = 0.04$		
	I_1	I_2	I_3	I_1	I_2	I_3
0	1.772454	1.253314	0.2453184	1.772454	1.253314	0.1859635
2	1.772454	1.253314	0.2455421	1.772454	1.253314	0.1829387
4	1.772454	1.253314	0.2098375	1.772454	1.253314	0.1900922
6	1.772454	1.253314	0.2065022	1.772454	1.253314	0.2083623
8	1.772454	1.253314	0.2010116	1.772454	1.253314	0.2204479
10	1.772454	1.253314	0.1748934	1.772454	1.253314	0.2350400

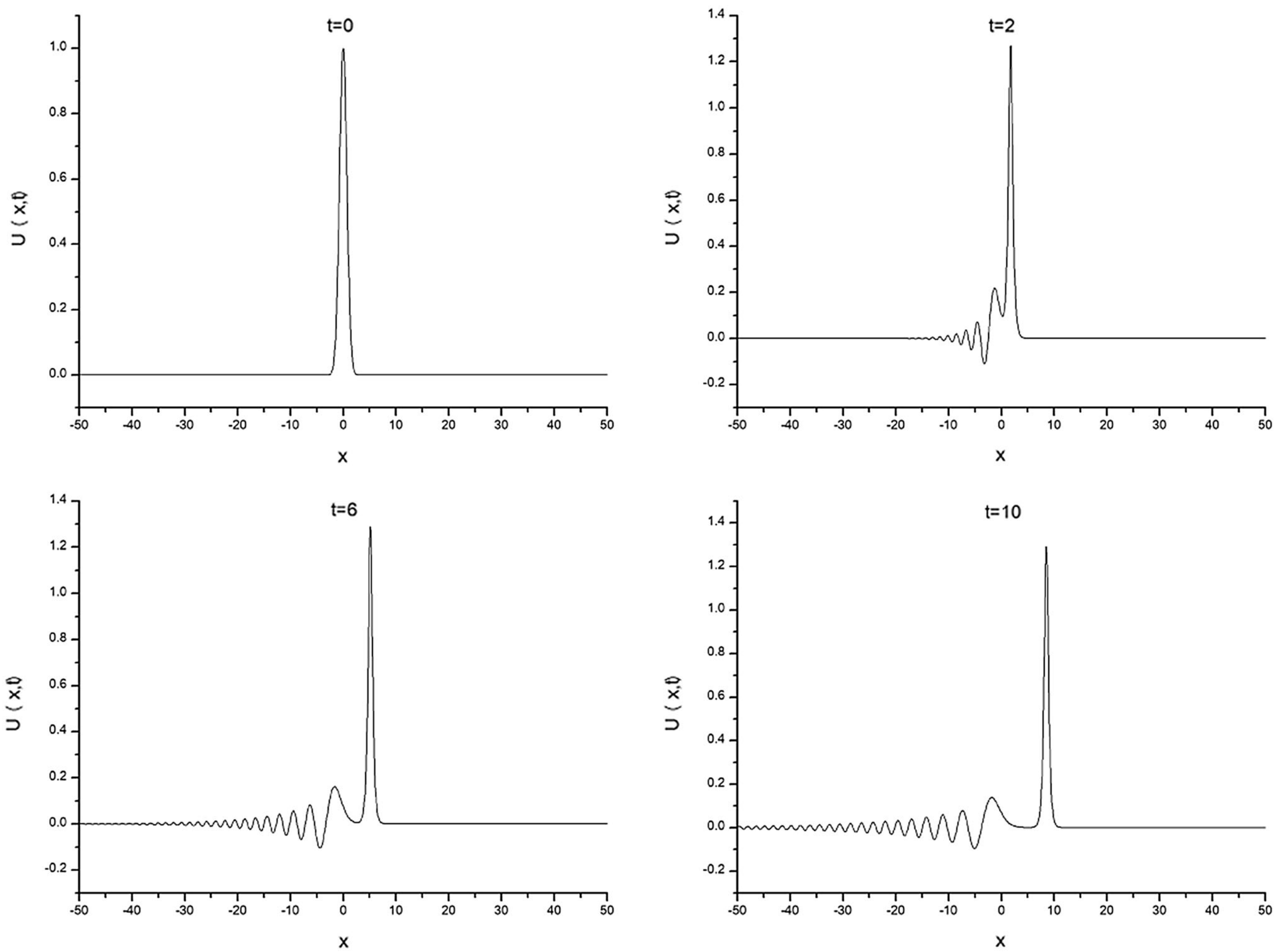

Fig. 8 Gaussian initial condition with $\varepsilon = 3$, $\mu = 0.1$, $h = 0.1$, $\Delta t = 0.01$ and $-50 \le x \le 50$ at $0 \le t \le 10$

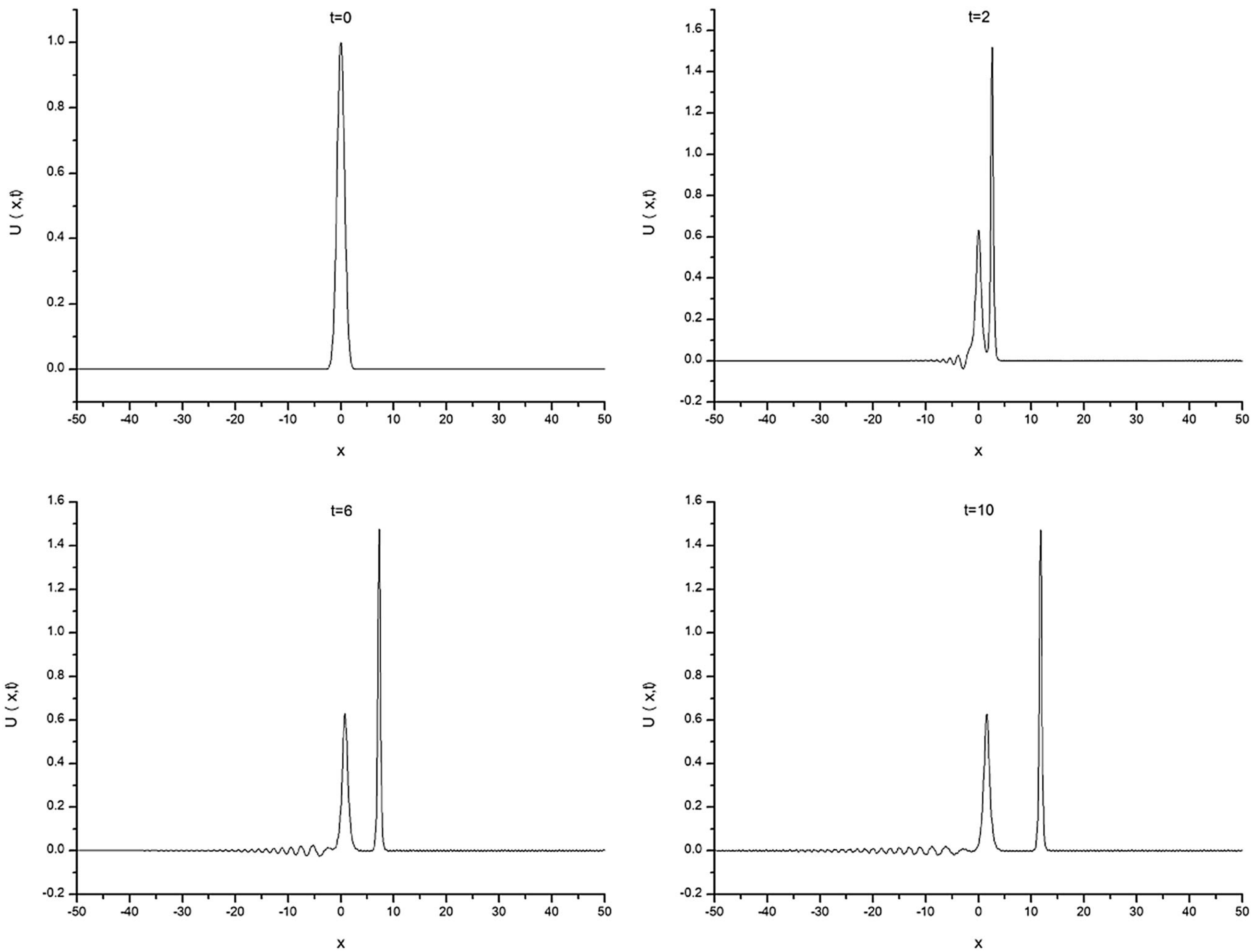

Fig. 9 Gaussian initial condition with $\varepsilon = 3$, $\mu = 0.04$, $h = 0.1$, $\Delta t = 0.01$ and $-50 \leq x \leq 50$ at $0 \leq t \leq 10$

between time $t = 6$ and $t = 20$ and waves started to resume their original shapes after the time $t = 20$.

6 Evolution of Solitons

Evolution of a train of solitons of the mKdV equation has been studied using the Gaussian initial condition

$$U(x,0) = \exp\left(-\mathrm{x}^2\right), \tag{40}$$

for various values of μ. In this case, the behavior of the solution depends on the values of μ. Therefore, the values of $\mu = 0.1$ and $\mu = 0.04$ are chosen at the region of the $-50 \leq x \leq 50$. The numerical computations are done up to $t = 10$. The values of the three invariants of motion for different μ are presented in Table 5. In addition, Figs. 8 and 9 illustrate the development of the Gaussian initial condition into solitary waves.

7 Conclusion

In this paper, a lumped Galerkin method based on cubic B-splines has been successfully applied to the mKdV equation to examine the motion of a single solitary wave, whose analytical solution is known, and extended the scheme to the study of two and three solitary waves, whose the analytical solution is unknown during the interaction. We have calculated the error norms L_2 and L_∞ and the conserved quantities to show how good and accurate the numerical solutions of the test problems. It has been observed that the error norms are satisfactorily small and the invariants are well conserved. The method successfully models the motion and interaction of the solitary waves and evolution of solitons. The obtained results indicate that the present method is more accurate than some earlier results found in the literature. As a result, we can say that lumped Galerkin method is more practical, accurate, and productive numerical approximation technique for mKdV equation and it can be reliably used to solve the similar type nonlinear problems.

Acknowledgements The author, Turgut Ak, is grateful to The Scientific and Technological Research Council of Turkey for granting scholarship for Ph.D. studies.

References

Biswas A (2010) 1-Soliton solution of Benjamin–Bona–Mahony equation with dual-power law nonlinearity. Commun Nonlinear Sci Numer Simul 15(10):2744–2746

Biswas A, Ismail MS (2010) 1-Soliton solution of the coupled KdV equation and Gear–Grimshaw model. Appl Math Comput 216(12):3662–3670

Biswas A, Raslan KR (2011) Numerical simulation of the modified Korteweg-de Vries equation. Phys Wave Phenom 19(2):142–147

Biswas A, Krishnan EV, Suarez P, Kara AH, Kumar S (2013) Solitary waves and conservation laws of Bona–Chen equations. Indian J Phys 87(2):169–175

Dyachenko S, Zakharov D, Zakharov V (2016) Primitive potentials and bounded solutions of the KdV equation. Physica D Nonlinear Phenom 333:148–156

Dutykh D, Tobisch E (2015) Direct dynamical energy cascade in the modified KdV equation. Physica D Nonlinear Phenom 297:76–87

Gheorghiu CI (2016) Stable spectral collocation solutions to a class of Benjamin Bona Mahony initial value problems. Appl Math Comput 273:1090–1099

Girgis L, Zerrad E, Biswas A (2010) Solitary wave solutions of the Peregrine equation. Int J Oceans Oceanogr 4(1):45–54

Greenwood C, Christie D, Venugopal V, Morrison J, Vogler A (2016) Modelling performance of a small array of wave energy coverters: comparison of spectral and Boussinesq models. Energy 113:258–266

Haq S, Hussian A, Islam S-U (2010) Solutions of coupled Burger's, fifth-order KdV and Kawahara equations using differential transform method with Padé approximantion. Selcuk J Appl Math 11(1):43–62

He B, Meng Q (2016) Three kinds of periodic wave solutions and their limit forms for a modified KdV-type equation. Nonlinear Dyn 86(2):811–822

Karakoc SBG, Zeybek H, Ak T (2014) Numerical solutions of the Kawahara equation by the septic B-spline collocation method. Stat Optim Inf Comput 2:211–221

Karakoc SBG, Ak T, Zeybek H (2014) An efficient approach to numerical study of the MRLW equation with B-spline collocation method. Abstr Appl Anal. Article ID 59640, 15 pages

Kaya D (2005) An application for the higher order modified KdV equation by decomposition method. Commun Nonlinear Sci Numer Simul 10(6):693–702

Korteweg DJ, de Vries G (1895) On the change of form of long waves advancing in a rectangular canal, and on a new type of long stationary wave. Philos Mag 39:422–443

Miura RM, Gardner CS, Kruskal MD (1968) Korteweg-de Vries equation and generalizations. II. Existence of conservation laws and constants of motion. J Math Phys 9(8):1204

Miura RM (1976) The Korteweg-de Vries equation: a survey of results. SIAM Rev 18(3):412–459

Prenter PM (1975) Splines and variational methods. Wiley, New York

Rashidi MM, Domairry G, Dinarvand S (2009) Approximate solutions for the Burger and regularized long wave equations by means of the homotopy analysis method. Commun Nonlinear Sci Numer Simul 14(3):708–717

Rashidi MM, Ganji DD, Dinarvand S (2009) Explicit analytical solutions of the generalized Burger and Burger–Fisher equations by homotopy perturbation method. Numer Methods Partial Differ Equ 25(2):409–417

Raslan KR, Baghdady HA (2015) A finite difference scheme for the modified Korteweg-de Vries equation. Gen Math Notes 27(1):101–113

Siddigi SS, Arshed S (2014) Quintic B-spline for the numerical solution of the good Boussinesq equation. J Egypt Math Soc 22(2):209–213

Shukla HS, Tamsir M, Srivastava VK, Kumar J (2014) Numerical solution of two dimensional coupled viscous Burger equation using modified cubic B-spline differential quadrature method. AIP Adv 4(117134):1–11

Triki H, Wazwaz A-M (2009) Sub-ODE method and soliton solutions for the variable-coefficient mKdV equation. Appl Math Comput 214(2):370–373

Triki H, Kara AH, Bhrawy AH, Biswas A (2014) Soliton solution and conservation law of Gear–Grimshaw model for shallow water waves. Acta Physica Polonica A 125(5):1099–1107

Triki H, Ak T, Moshokoa S, Biswas A (2016) Soliton solutions to KdV equation with spatio-temporal dispersion. Ocean Eng 114:192–203

Ueckermann MP, Lermusiaux PFJ (2016) Hybridizable discontinuous Galerkin projection methods for Navier–Stokes and Boussinesq equations. J Comput Phys 306(1):390–421

Vaneeva O, Popovych RO, Sophocleous C (2015) Group analysis of Benjamin–Bona–Mahony equations with time dependent coefficients. J Phys Confer Ser 621:1–12

Wazwaz A-M (2008) New travelling wave solutions to the Boussinesq and the Klein–Gordon equations. Commun Nonlinear Sci Numer Simul 13(5):889–901

Wazwaz A-M, Triki H (2011) Soliton solutions for a generalized KdV and BBM equatitons with time-dependent coefficients. Commun Nonlinear Sci Numer Simul 16(3):1122–1126

Wazwaz A-M (2012) (2+1-dimensional mKdV(N) equations by the mKdV recursion operator: multiple soliton and multiple singular soliton solutions. Appl Math Comput 219(5):2535–2544

Wazwaz A-M, Xu G-Q (2015) Negative-order modified KdV equations: multiple soliton and multiple singular soliton solutions. Math Methods Appl Sci 39(4):661–667

Wazwaz A-M (2016) The simplified Hirotas method for studying three extended higher-order KdV-type equations. J Ocean Eng Sci 1(3):181–185

Zeybek H, Karakoc SBG (2016) A numerical investigation of the GRLW equation using lumped Galerkin approach with cubic B-spline. SpringerPlus 5(199):1–17